

Implementation of multi-walker quantum walks with cavity grid

Peng Xue

Department of Physics, Southeast University, Nanjing 211189 China

(Dated: October 25, 2018)

We show how multi-walker quantum walks can be implemented in a quantum quincunx created via cavity quantum electrodynamics. The implementation of a quantum walk with a multi-walker opens up the interesting possibility to introduce entanglement and more advanced walks. With different coin tosses and initial states the multi-walker quantum walk shows different probability distributions which deviate strongly from the classical random walks with quadratic enhanced spreadings and localization effects. By introducing decoherence, the transition from quantum walks to the classical versions is observed. We introduce the average fidelity decay as a signature to investigate the decoherence-induced irreversibility of quantum walks.

PACS numbers: 03.67.Ac, 42.50.Pq, 74.50.+r

I. INTRODUCTION

Quantum walks (QWs) [1] offer an alternative approach to implement quantum algorithms [2] compared to the typical circuit-based [3] or measurement based [4] models for quantum algorithms. There are two types of QWs: the continuous time QWs [5] and the discrete time QWs [6]. The realization for QWs have been proposed in quantum optics [7], ion trap [8, 9], cavity quantum electrodynamics (QED) [10, 11] and optical lattice [12] systems in a decade. QWs on single photons [13], trapped ions [14] and neutral atoms [15] have been realized in the laboratory, respectively. More recently, higher dimensional QWs [16] and QWs involving more particles [17–24] are studied. This reveals the additional features offered by quantum mechanics, such as quantum correlations [24] and indistinguishability. Compared to the proposals on QWs with single-walker, we extend the QWs by using multi-walker. The implementation of a QW with a multi-walker opens up the interesting possibility to introduce entanglement and more advanced walks.

To create a QW, the following steps are followed: a particular QW is chosen, in our case a discrete multi-walker QW with joint coins each of which decides to the corresponding walker's position shifts. Furthermore, a signature for QW behavior is identified, such as enhanced diffusion or uniformity of the distribution for the walkers' degree of freedom. Then a physical system is chosen whose Hamiltonian dynamics match the evolution of the QW. Finally, open system dynamics are incorporated into the analysis in order to account for non-unitary evolution as well as to incorporate realistic measurement into the model.

Compared to random walks (RWs), QWs are reversible. The irreversibility due to decoherence transmits the QW to RW. It is of great interest to show the variation of the irreversibility in the time evolution of the QW. The probability distribution and standard deviation of the distribution are used to study the irreversibility of QWs in the present of decoherence. However those approaches are not operational. That means neither of them provides a way for direct experimental obser-

vation of the irreversibility of the QW. In the present of decoherence, except for the probability distribution and the standard deviation, we introduce an operational measurement—the average fidelity decay (AFD) [25, 26]. The AFD can reveal the response of the system to the decoherence which is closely related to the properties of both the system and the environment, and provide an experimentally available way to monitor the detrimental influence on the QW with different decoherence sources.

II. QUANTUM WALKS WITH ONE- AND MULTI-WALKER

Let us first briefly review a single-walker QW. The Hilbert space of the walker+coin is given by a tensor product

$$\mathcal{H} = \mathcal{H}_w \otimes \mathcal{H}_c \quad (1)$$

of the walker space \mathcal{H}_w and the two-dimensional (2D) coin space

$$\mathcal{H}_c = \text{span}\{|-1\rangle, |1\rangle\}. \quad (2)$$

We consider a walker starting the QW from the origin, i.e., the initial state has the form

$$|\psi\rangle_{\text{ini}} = |\psi_0\rangle_w \otimes |\psi\rangle_c, \quad (3)$$

where $|\psi_0\rangle_w$ and $|\psi\rangle_c$ denote the initial state of the walker and coin respectively. After N steps of the QW, the state of the walker+coin is given by

$$\begin{aligned} |\psi_N\rangle &= U^N |\psi\rangle_{\text{ini}} \\ &= \sum_j p_{-1}(j, N) |\psi_j\rangle_w |-1\rangle + p_1(j, N) |\psi_j\rangle_w |1\rangle, \end{aligned} \quad (4)$$

where the unitary propagator U has the form

$$U = S(\mathbb{I} \otimes C). \quad (5)$$

The probability distribution generated by the QW is given by

$$p(j, N) = \left| \langle \psi_j | \langle -1 | \psi_N \rangle \right|_{\text{w}}^2 + \left| \langle \psi_j | \langle 1 | \psi_N \rangle \right|_{\text{w}}^2 = \left| p_{-1}(j, N) \right|^2 + \left| p_1(j, N) \right|^2. \quad (6)$$

The coin operator C flips the state of the coin before the walker is displaced. In principle, C can be an arbitrary unitary operation on the coin space \mathcal{H}_c . We choose the most studied case of the Hadamard coin, denoted by $H = \begin{pmatrix} 1 & 1 \\ 1 & -1 \end{pmatrix} / \sqrt{2}$, which is defined by its action on the basis states,

$$H |\pm 1\rangle = (|-1\rangle \mp |1\rangle) / \sqrt{2}. \quad (7)$$

After the coin flip, the step operator S displaces the walker from its current state according to its coin state

$$S |\psi_j\rangle_{\text{w}} |\pm 1\rangle \longrightarrow |\psi_j \pm \delta\rangle_{\text{w}} |\pm 1\rangle, \quad (8)$$

where δ is the step size. The coefficients $p_{\pm 1}(j, N)$ represent the probability amplitudes of finding the walker at $|\psi_j\rangle_{\text{w}}$ after N steps of the QW with the coin state $|\pm 1\rangle$.

As an extension, we choose the N -walker QW over circles in phase space, which arises naturally for N harmonic oscillators. Points in phase space correspond to the oscillator position-momentum pair (x, p) , which we henceforth refer to as the phase space ‘location’.

For the discrete N -walker QW on the circles, each of the walker’s location as a point in phase space is replaced by a localized wavefunction centered at location (x, p) , and the random flips are replaced by joint quantum coins given by qubits, which are flipped by a unitary operation and then entangled with the oscillators by free evolution. An example of N -walker state is the product state

$$|\psi\rangle_{\text{w}} = |\phi_1\rangle \otimes |\phi_2\rangle \otimes \dots \otimes |\phi_N\rangle. \quad (9)$$

An example of the coin state is $|\psi\rangle_c = |c_1, c_2, \dots, c_N\rangle$. The archetypal discrete time N -walker QW consists of two building blocks—a coin operator C and a step operator S . The coin is essentially an ancillary parameter that is used by the step operator to decide how to propagate the walker. The simplest example of the coin operation is to apply a Hadamard transformation to each qubit in the decomposition of Eq. (9). This internal transformation is separable, in the sense that it does not produce entanglement between the spatial degree of freedom. Other choices for the coin operations include the entangling coin operation, the discrete Fourier transform (DFT) and the Grover operation. A common choice of step operator is

$$S |\psi\rangle_{\text{w}} |\psi\rangle_c = |\phi_1 + c_1\delta\rangle \otimes |\phi_2 + c_2\delta\rangle \otimes \dots \otimes |\phi_N + c_N\delta\rangle |c_1, c_2, \dots, c_N\rangle, \quad (10)$$

where $c_i \in \{-1, 1\}$ and

$$|\phi_j\rangle = \frac{1}{\sqrt{M}} \sum_{n=0}^M e^{i\phi_j n} |n\rangle \quad (11)$$

for $j = 1, \dots, N$ is the phase state.

Using two-walker QW as an example, one obvious generalization of coin tossing operations is to apply a Hadamard transformation H to each qubit of the coin state. This choice can be viewed as two independent coin tosses on each qubit of the coin state. The transformation is

$$C_1 = H \otimes H = \frac{1}{2} \begin{pmatrix} 1 & 1 & 1 & 1 \\ 1 & -1 & 1 & -1 \\ 1 & 1 & -1 & -1 \\ 1 & -1 & -1 & 1 \end{pmatrix}. \quad (12)$$

This coin operation is separable, in the sense that it does not produce entanglement between the spatial degrees of freedom.

In principle, any unitary transformations on the coin state can replace Hadamard transformation and be used as coin tosses. Now we introduce non-separated coin tosses. One obvious generalization of coin tosses, which is not separable and does produce entanglement between the coin qubits, is the root of SWAP gate operation, defined as follows

$$C_2 = \sqrt{i\text{SWAP}} = \begin{pmatrix} 1 & 0 & 0 & 0 \\ 0 & \cos \theta & i \sin \theta & 0 \\ 0 & i \sin \theta & \cos \theta & 0 \\ 0 & 0 & 0 & 1 \end{pmatrix}. \quad (13)$$

Another choice of non-separated ncoin tosses—the discrete Fourier transform (DFT) D , defined as follows:

$$C_3 = D = \frac{1}{2} \begin{pmatrix} 1 & 1 & 1 & 1 \\ 1 & i & -1 & -i \\ 1 & -1 & 1 & -1 \\ 1 & -i & -1 & i \end{pmatrix} \quad (14)$$

transforms any coin translation eigenstate into an equally weighted superposition of all the eigenstates and entangles the spatial degrees of freedom of coin qubits.

There are, of course, an infinite variety of other non-separable choices for the coin tosses by employing different phase relationships. Finally we introduce the Grover operator as a non-separated coin toss defined as follows

$$C_4 = G = \frac{1}{2} \begin{pmatrix} -1 & 1 & 1 & 1 \\ 1 & -1 & 1 & 1 \\ 1 & 1 & -1 & 1 \\ 1 & 1 & 1 & -1 \end{pmatrix}. \quad (15)$$

We now investigate the effect of measurement on a two-walker system. After k th steps of two-walker QW, the state of the walker+coin system becomes $|\psi_k\rangle = (SC)^k |\psi_{\text{ini}}\rangle$. Suppose we perform a measurement and detect the first (second) walker at position ϕ . Then the state will be projected into

$$P_{1(2)}(\phi) = \langle \phi | \text{Tr}_{1(2)} \rho_{\text{w}} | \phi \rangle, \quad (16)$$

where $\rho_{\text{w}} = \text{Tr}_c(|\psi_k\rangle \langle \psi_k|)$.

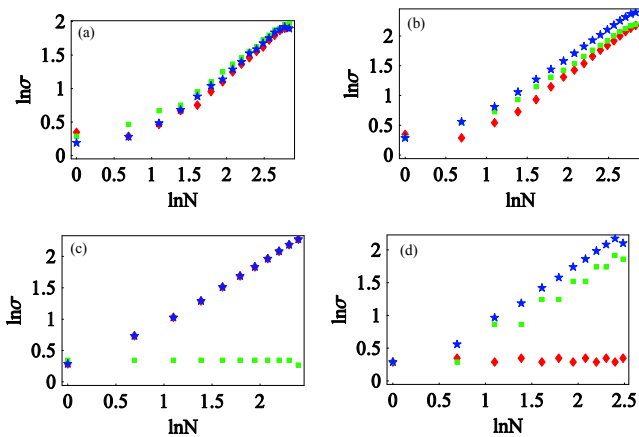


FIG. 1: (Color online.) The ln-ln plot of the position spreads $\sigma(\phi)$ of the first walker taking the ideal two-walkers QWs with different coin tosses (a) DFT D , (b) $H \otimes H$, (c) \sqrt{i} SWAP and (d) Grover G as functions of the position ϕ for different initial coin states $|\Psi\rangle_{c1} = (|1\rangle + |-1\rangle) \otimes (|1\rangle + |-1\rangle)/2$ (\blacklozenge), $|\Psi\rangle_{c2} = |1\rangle \otimes |1\rangle$ (\blacksquare) and $|\Psi\rangle_{c3} = (|1\rangle + i|-1\rangle) \otimes (|1\rangle + i|-1\rangle)/2$ (\star).

$s \pm \Delta s$	$ \psi\rangle_{c1}$	$ \psi\rangle_{c2}$	$ \psi\rangle_{c3}$
D	0.940 ± 0.003	0.880 ± 0.002	0.887 ± 0.003
$H \otimes H$	0.979 ± 0.005	0.897 ± 0.007	0.994 ± 0.004
\sqrt{i} SWAP	0.965 ± 0.001	0	0.965 ± 0.001
G	0	0.911 ± 0.002	0.973 ± 0.006

TABLE I: Linear regression results for $\ln \sigma(\phi) = (s \pm \Delta s) \ln N$ for the ideal case with the step size $\delta = 0.8$ in ln-ln scale shown in Fig. 1.

The dispersion of the distribution (16) is especially important. As moments are not particularly useful for distributions over compact domains, other strategies are needed. For the phase distribution over the domain $[0, 2\pi]$, Holevo's version [27] of the standard deviation

$$\sigma(\phi) = \sqrt{\left| \int_0^{2\pi} d\phi P(\phi) e^{i\phi} \right|^{-2} - 1} \quad (17)$$

is particularly useful as it reduces to the ordinary standard deviation for small spreads and is sensible when the dispersion is large over the domain.

We begin our analysis the results of two-walker QW with different coin tosses. The initial conditions for the coin state were chosen to be the separable state composed of all qubits in the states $|1\rangle$, $(|1\rangle + |-1\rangle)/\sqrt{2}$, and $(|1\rangle + i|-1\rangle)/\sqrt{2}$, which lead to three different probability distributions.

For the case of separable transformation with separable initial conditions, the different walkers behave independently; thus, the variance can be expressed in terms of one-walker case. Furthermore, a bias could be introduced into the transformation and give a different weighted superposition of translation eigenstates. Thus the phase distribution of walker also depends on the initial state of

the coin. The time dependence of the standard deviation for QW is plotted in Fig. 1 and the corresponding slopes $\Delta\sigma/\Delta t$ ($\ln \sigma(\phi)/\ln N$) are presented in Table I. We observe that the standard deviation for QW with the same coin toss depends on the symmetry of the initial states. However the quantum behavior can always be observed except for the two cases—the \sqrt{i} SWAP QW with the initial coin state $|1\rangle \otimes |1\rangle$ and the Grover G QW with the initial coin state $(|1\rangle + |-1\rangle) \otimes (|1\rangle + |-1\rangle)/2$, which shows the localization effect on QW where the walker's spread becomes constant [28, 29].

Any real implementation of a quantum system must deal with the issue of decoherence, which tends to destroy quantum correlations. The entanglement decay due to noise leads the transition from QWs to RWs. In the present of decoherence, except for the probability distribution and the standard deviation of the distribution another operational measurement here is introduced as a new signature for QWs. We measure the irreversibility of the QW due to decoherence by the AFD which is defined based on fidelity decay, that is the square modulus of the overlap between two time dependent final states with the same initial state under the time evolution without and with decoherence respectively. The AFD [26] is defined as

$$AFD = \text{Tr}[\rho(t) |\Psi_N\rangle \langle \Psi_N|], \quad (18)$$

where $\rho(t)$ is the density matrix of the walker+coin system after the time evolution. The AFD reveals the response of the walker+coin system to the decoherence and is sensitive to different sources of decoherence.

III. IMPLEMENTATION OF MULTI-WALKER QWS ON CIRCLES

Multi-walker QWs can be implemented with scalable cavity grid [30] with superconducting circuits [31, 32]. The walkers are represented by the cavity modes and the coin states $\{|-1\rangle, |1\rangle\}$ are encoded with charge qubits. The cavity grid consists of cavity modes belonging to N_H horizontal (H) and N_V vertical (V) cavities, $\hat{H}_{\text{cav}} = \sum_{j=1}^{N_H} \omega_j^H \hat{a}_j^\dagger \hat{a}_j + \sum_{j=1}^{N_V} \omega_j^V \hat{b}_j^\dagger \hat{b}_j$, coupled to one charge qubit at each intersection (i, j) , generalizing to a 2D architecture:

$$\hat{H}_{\text{cav-qb}} = \sum_{i,j} |1\rangle_{ij} \langle 1| \left[g_{ij}^H (\hat{a}_i + \hat{a}_i^\dagger) + g_{ij}^V (\hat{b}_j + \hat{b}_j^\dagger) \right]. \quad (19)$$

The coupling $g_{ij}^{H(V)}$ between the horizontal (vertical) cavity mode i (j) and the charge qubits is switchable by the external electric field on each charge qubit [33]. Eq. (19) leads to the Jaynes-Cummings (JC) model and the cavity-mediated interaction between qubits.

For a multi-walker QW, one can implement the coin operation on charge qubits capacitively coupled to a vertical cavity mode (j) with cavity-assisted interaction.

The conditional position shifts of each walker can be implemented for each horizontal cavity mode i under the free evolution of the JC interactions between horizontal cavity mode i and charge qubit (i, j) .

The multi-walker QW with cavity grid can be implemented by steps as follows. Step I, the state of the cavity grid is prepared in a certain initial state. Step II, the couplings between the vertical cavity mode and the charge qubits are turned on to implement the coin operation on charge qubits with cavity-assisted interactions. Step III, the couplings between the vertical cavity mode and the charge qubits are turned off and those between the horizontal cavity modes and the charge qubits are turned on to implement the conditional position shifts of each walker due to the coin states. Then, we repeat steps II and III for the next step of multi-walker QW.

A. The Conditional Phase Shifts

Using a two-walker QW as an example, we consider a system including two two-level charge qubit coupled to a cavity grid with the structure mentioned above. The coupling between each charge qubit and the corresponding horizontal cavity field is used to implement conditional phase shifts on circles and the charge states are used to implement quantum coins, each of them with two possible operations. The physical implementation of the conditional phase shifts of multi-walker quantum walks can be implemented by the free-evolution of the cavity-assisted interaction Eq. (19), which can be rewritten in the JC model [31]

$$\hat{H}_{\text{JC}} = \sum_{j=1,2} \left[\omega_c \hat{a}_j^\dagger \hat{a}_j + \frac{\omega_a}{2} \hat{\sigma}_z^j + g(\hat{a}_j^\dagger \hat{\sigma}_-^j + \hat{a}_j \hat{\sigma}_+^j) \right] \quad (20)$$

with ω_a and ω_c the coin and cavity frequencies, respectively, and g the coupling strength. In the dispersive regime,

$$|\Delta| = |\omega_a - \omega_c| \gg g, \quad (21)$$

and in a rotating frame, the effective interaction Hamiltonian is

$$\hat{H}_{\text{int}} = \sum_{j=1,2} \chi \hat{a}_j^\dagger \hat{a}_j \hat{\sigma}_z^j \quad (22)$$

with the cavity pull of the resonator

$$\chi = \frac{g^2}{\Delta}. \quad (23)$$

After the coin flipping operation, the time evolutions of the interactive Hamiltonian give the conditional position shifts due to the charge states

$$U_j = \exp(i\Delta\theta_j \hat{a}_j^\dagger \hat{a}_j \hat{\sigma}_z^j), \quad (24)$$

for $j = 1, 2$, where $\Delta\theta_{1(2)}$ is the size of one step for walker 1(2) which depends on the effective coupling χ and the time duration $t_{1(2)}$.

B. The Coin Tosses

1. The Separable Coin Toss

The coin tosses can be implemented on charge qubits with cavity-assisted interactions. Now we turn off the couplings between the charge qubits and the horizontal cavities. Then we turn on the coupling between the charge qubits and the vertical cavity subsequently. The time-dependent driving field applying on the vertical cavity [31]

$$\hat{H}_d = \epsilon(t) (\hat{b}^\dagger e^{-i\omega_d t} + \hat{b} e^{i\omega_d t}) \quad (25)$$

can be used to implement the separable coin toss. It is sufficient to let $\epsilon(t)$ be a square wave so ϵ is a constant ($\epsilon = 0$ when the field is off). In the dispersive regime and in a frame rotating at ω_d for the qubit and the resonator, $\hat{H}_j = \hat{H}_{\text{JC}}^j + \hat{H}_d$ can be replaced by the effective Hamiltonian

$$\hat{H}_{1q}^j = \chi \hat{b}^\dagger \hat{b} \hat{\sigma}_z^j - \frac{\delta_{da}}{2} \hat{\sigma}_z^j + \frac{\Omega_R}{2} \hat{\sigma}_x^j - \delta_{dc} \hat{b}^\dagger \hat{b} + \epsilon(\hat{b}^\dagger + \hat{b}) \quad (26)$$

with

$$\delta_{da} = \omega_d - \omega_a, \delta_{dc} = \omega_d - \omega_c, \quad (27)$$

$$\Omega_R = \frac{2g\epsilon}{\delta_{dc}} \quad (28)$$

the Rabi frequency.

The first term in the above expression effects the coin-induced walker phase shift. The atom transition is an ac-Stark shifted by $g^2 \hat{b}^\dagger \hat{b} \Delta$. To implement

$$H \otimes H = \Pi_{j=1,2} \exp[i t_H \Omega_R \hat{\sigma}_x^j / 2] \quad (29)$$

on the coin, we choose

$$\omega_d = \frac{2\bar{n}g^2}{\Delta} - \frac{2g\epsilon}{\Delta} + \omega_a \quad (30)$$

with pulse duration $t_H = \pi/2\Omega_R$.

After the coin flipping we shut off both the external field and the coupling between the charge qubits and the vertical cavity, and turn on the coupling between the charge qubits and the horizontal cavities. The free evolution continues for a duration t_j for charge qubit j for the conditional phase shifts.

2. The \sqrt{i} SWAP Coin Toss

If one turn on the couplings between the two charge qubits and the vertical cavity at the same time, the effective Hamiltonian of \hat{H}_{JC} can be written as

$$\begin{aligned} \hat{H}_{2q} = & (\omega_c + \chi \sum_{j=1,2} \hat{\sigma}_z^j) \hat{b}^\dagger \hat{b} + \frac{1}{2} (\omega_a + \chi) \sum_{j=1,2} \hat{\sigma}_z^j \\ & + \chi (\hat{\sigma}_+^1 \hat{\sigma}_-^2 + \hat{\sigma}_-^1 \hat{\sigma}_+^2). \end{aligned} \quad (31)$$

The forth term is the induced dipole-dipole interaction between the two charge qubits, which can be used to implement the $\sqrt{-i\text{SWAP}}$ coin toss on the charge states

$$\sqrt{-i\text{SWAP}} = \begin{pmatrix} 1 & 0 & 0 & 0 \\ 0 & \cos \theta & -i \sin \theta & 0 \\ 0 & -i \sin \theta & \cos \theta & 0 \\ 0 & 0 & 0 & 1 \end{pmatrix} \quad (32)$$

with $\theta = \chi t_s$ and t_s the evolution time of (31)

$$U_{2q} = \exp \left[-i\theta (\hat{b}^\dagger \hat{b} + \frac{1}{2}) \sum_{j=1,2} \hat{\sigma}_z^j \right] \sqrt{i\text{SWAP}}. \quad (33)$$

3. The DFT Coin Toss

The similar system can be used to implement a 2D discrete Fourier transform (DFT) coin toss, defined in Eq. (14). Note that the Hadamard transformation is the 1D DFT [34].

For the coin flipping, if we choose the duration t_j to increase geometrically with qubit number as $\chi t_j = 2^j \pi/4$, then the Hamiltonian $\hat{H}_{\text{int}}^j = \chi \hat{b}^\dagger \hat{b} \hat{\sigma}_z^j$ generate a unitary transformation

$$D = \exp \left(\frac{-i\pi \hat{b}^\dagger \hat{b} \hat{\Upsilon}}{2} \right), \quad (34)$$

where the electronic operator $\hat{\Upsilon}$ provides a binary ordering of the qubits:

$$\hat{\Upsilon} = \sum_{j=1,2} 2^{j-1} \hat{\sigma}_z^j. \quad (35)$$

The eigenvectors of the operator $\hat{\Upsilon}$ are the electronic number states

$$\hat{\Upsilon} = \sum_{k=0}^3 k |k\rangle \langle k|, \quad (36)$$

where $|k\rangle = |S_N\rangle_N \otimes |S_{N-1}\rangle_{N-1} \otimes \dots \otimes |S_1\rangle_1$, $S_j = 0, 1$ and $k = S_N^{N-1} + S_{N-1} \times 2^{N-2} + \dots + S_1 \times 2^0$. The binary expansion for k is thus just the string $S_N S_{N-1} \dots S_1$.

This unitary operation can be used to implement a 2D DFT shown in Eq. (14). First we turn on the coupling between charge qubit 1 and the vertical cavity and after time duration t_1 it is turned off. Then we turn on that between charge qubit 2 and the vertical cavity and after time duration t_2 it is turned off. Thus the DFT operation on two charge qubits is realized.

4. The Grover Coin Toss

The induced dipole-dipole interaction between two charge qubits can be used to implement the Grover coin

toss [35]. Now we turn on the coupling between the charge qubits and the vertical cavity at the same time and apply a drive field (25) on the vertical cavity. The effective Hamiltonian of the system in the dispersive limit becomes

$$\begin{aligned} \hat{H}'_{2q} = \sum_{j=1,2} & (\chi \hat{b}^\dagger \hat{b} \hat{\sigma}_z^j - \frac{\delta_{\text{da}}}{2} \hat{\sigma}_z^j + \frac{\Omega_R}{2} \hat{\sigma}_x^j) \\ & + \chi (\hat{\sigma}_+^1 \hat{\sigma}_-^2 + \hat{\sigma}_-^1 \hat{\sigma}_+^2) - \delta_{\text{dc}} \hat{b}^\dagger \hat{b} + \epsilon (\hat{b}^\dagger + \hat{b}). \end{aligned} \quad (37)$$

If $\Omega_R \gg \delta_{\text{da}}, \delta_{\text{dr}}, g$, we can get the time evolution of the system in the interaction picture

$$U_I(t) = e^{-i\hat{H}_0 t} e^{-i\hat{H}_e t} \quad (38)$$

with

$$\hat{H}_0 = \Omega_R/2 \sum_{j=1,2} \hat{\sigma}_x^j \quad (39)$$

$$\hat{H}_e = \chi (\hat{\sigma}_1^\dagger \hat{\sigma}_2^\dagger + \hat{\sigma}_1^\dagger \hat{\sigma}_2^-) + h.c..$$

For choosing $\chi t = \pi/8$ and $\Omega_R/\chi = 16m + 4$ for m an integer, we can get

$$U_I(t) = -G. \quad (40)$$

So by choosing appropriate values of parameters, we can generate a two-qubit Grover operation on two charge qubits.

The multi-walker QWs can be implemented by three steps as follows. First, the cavity grid is prepared in the initial state $|\Psi\rangle_{\text{ini}}$. Second, we turn off the couplings between the charge qubits and the corresponding horizontal cavity modes and turn on those between the charge qubits and vertical cavity. We applies a coin flipping operation on the charge state. Third, we turn off the coupling between the charge qubits and vertical cavity and turn of those with horizontal ones and the free evolution of the interaction between the charge qubits and cavity modes is used to implement the conditional phase shift for one step of QW.

IV. OPEN SYSTEM

Coupling to additional uncontrollable degree of freedom leads to energy relaxation and dephasing in the system. In the Born-Markov approximation, these effects can be characterized by a cavity photon leakage rate κ and a pure dephasing rate γ for each qubit of the coin state. The open system thus evolves according to

$$\frac{\partial \rho}{\partial t} = -i[\hat{H}_{\text{int}}, \rho] + \sum_{j=1,2} \kappa_j \mathcal{D}[\hat{a}_j] \rho + \frac{\gamma_j}{2} \mathcal{D}[\hat{\sigma}_z^j] \rho \quad (41)$$

with

$$\mathcal{D}[\hat{L}] \rho \equiv \frac{1}{2} (2\hat{L} \rho \hat{L}^\dagger - \hat{L}^\dagger \hat{L} \rho - \rho \hat{L}^\dagger \hat{L}). \quad (42)$$

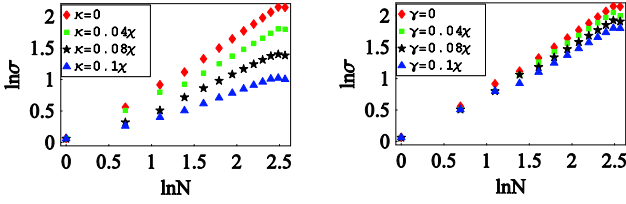


FIG. 2: (Color online.) The $\ln\text{-}\ln$ plot of the phase spreads $\sigma(\phi)$ of the three-side coin QWs implemented in cavity QED with the DFT coin tosses and step size $\Delta\theta = 0.8$ as functions of the phase ϕ for the initial coin states $(|1\rangle + i|-1\rangle) \otimes (|1\rangle + i|-1\rangle)/2$ with the presence of decoherence. (a) Fixing the dephasing rate $\gamma = 0.06\chi$, one can observe the QW-RW transition by increasing the cavity decay rate from $\kappa = 0$ to $\kappa = 0.1\chi$. (b) Fixing the decay rate $\kappa = 0.01\chi$, the slope of $\ln\text{-}\ln$ plot decreases slowly with γ/χ increasing.

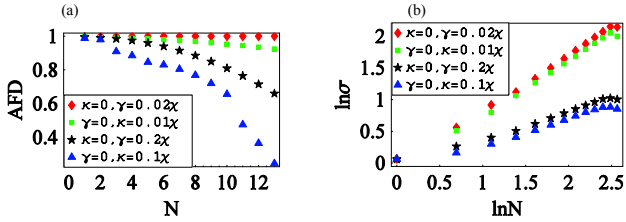


FIG. 3: (Color online.) With the step size $\Delta\theta = 0.8$, (a) AFDs and (b) $\ln\text{-}\ln$ plot of the phase spreads $\sigma(\phi)$ of the three-side coin QWs implemented in cavity QED with the DFT coin tosses as functions of the phase ϕ for the initial coin states $(|1\rangle + i|-1\rangle) \otimes (|1\rangle + i|-1\rangle)/2$ in the presence of decoherence.

The master equation is used to compute $\rho(t)$ from which the reduced state of the walker $\rho_w = \text{Tr}_c \rho$ is obtained. As a signature of QWs the phase distribution can be obtained by performing full optical homodyne tomography on the cavity to obtain the Wigner function, and hence the standard deviation thereby can be determined.

With the realistic system parameters [31, 32] $(\omega_a, \omega_c, g, \epsilon)/2\pi = (7000, 5000, 100, 1000)\text{MHz}$, simulated evolutions of the standard deviations of the phase distribution for the first several steps are presented in Fig. 2, which clearly reveal slope compatible with the characteristic quadratic decrease in phase spreading for increasing decoherence of the two-walker QW until the transition to the RW [36]. Here we use a DFT coin QW with initial coin state $(|1\rangle + i|-1\rangle) \otimes (|1\rangle + i|-1\rangle)/2$ as an example with the decay rate of cavity $\kappa_1 = \kappa_2$ increasing from 0 to 0.1χ and the dephasing rate $\gamma_1 = \gamma_2 = 0.06\chi$ fixed. Thus the QW-RW transition is observed in Fig. 2(a). Furthermore, if the decay rate $\kappa_1 = \kappa_2 = 0.01\chi$ is fixed, with the dephasing rate increasing the standard deviation of the phase distribution σ as a function of the number of steps N decreases slowly. And with γ increasing from 0 to 0.1χ the slope of the $\ln\sigma\text{-}\ln N$ plot decreases from 0.970 to 0.810 in Fig. 2(b).

Except for the standard deviation of the probability distribution, one can determine the effects of the deco-

herence on the quantum behavior of QWs via the AFD. As shown in Fig. 3(a), we have numerically calculated the AFD of the DFT coin QW with the initial coin state $(|1\rangle + i|-1\rangle) \otimes (|1\rangle + i|-1\rangle)/2$ in the two cases: (i) only with the decay of the cavity; (ii) only with the dephasing of the charge qubits. Using the parameters with which the standard deviations in the presence of the two sources of decoherence are quite close shown in Fig. 3(b), one can observe that the AFDs of the two cases are quite different and the difference increases with the decoherence increasing. In Fig. 3(b), the $\ln\sigma\text{-}\ln N$ plots are shown with different parameters. The result with $\kappa_1 = \kappa_2 = 0$ and $\gamma_1 = \gamma_2 = 0.02\chi$ ($\kappa_1 = \kappa_2 = 0$ and $\gamma_1 = \gamma_2 = 0.2\chi$) is quite similar with that with $\gamma_1 = \gamma_2 = 0$ and $\kappa_1 = \kappa_2 = 0.01\chi$ ($\gamma_1 = \gamma_2 = 0$ and $\kappa_1 = \kappa_2 = 0.1\chi$). Whereas, in Fig. 3(a) with the same choices of parameters, the AFDs are quite different and derive from each other. The AFD is more sensitive to the cavity decay rather than to the charge dephasing. These results imply the significant effect on the QW-RW transition from the cavity decay κ . Moreover, the cavity decay κ is much more important than the charge dephasing γ with respect to the scaling of AFD with time t (proportional to the number of steps N). The dephasing rate γ mainly leads to smearing the phase distribution and the phase distribution loses its symmetry.

V. CONCLUSION

In summary, we have introduced a protocol to implement a QW with a multi-walker in phase space using cavity QED. The implementation of a QW with a multi-walker opens up the interesting possibility to introduce entanglement and more advanced walks. With different coin tosses and initial states the multi-walker QWs show different probability distributions which deviate strongly from the RWs and show faster spreadings and localization effect. By introducing decoherence, the transmission from QWs to the classical versions is observed. We propose a physical realization to investigate the decoherence-induced irreversibility of QWs via the AFD. Our scheme provides an experimentally available way to monitor the detrimental influence on the QW by different decoherence sources. It is observed that the cavity decay has more detrimental effects on QWs rather than the dephasing of the charge qubits, which allows us to understand better the QW simulation in a realistic system. In conclusion, our theory establishes a pathway to realizing a many-step QW with multi-walker, and our techniques for observing the signature of QW via the AFD would be useful for general quantum information protocols.

Acknowledgments

This work has been supported by the National Natural Science Foundation of China under Grant Nos 11004029

and 11174052, the Natural Science Foundation of Jiangsu Province under Grant No BK2010422, the Ph.D. Programs Foundation of Ministry of Education of China, the Excellent Young Teachers Program of Southeast Uni-

versity and the Major State Basic Research Development Program of China (973 Program) under Grant No 2011CB921203.

-
- [1] Y. Aharonov, L. Daviovich and N. Zagury, *Phys. Rev. A* **48**, 1687 (1993).
 - [2] D. Aharonov, A. Ambainis, J. Kempe and U. Vazirani, *Proc. 33th STOC (New York)* pp 50-59 (2000).
 - [3] M. A. Nielsen and I. L. Chuang, *Quantum Computation and Quantum Information* (Cambridge: Cambridge University Press) (2000).
 - [4] R. Raussendorf and H. J. Briegel, *Phys. Rev. Lett.* **86**, 5188 (2001).
 - [5] A. M. Childs, *Phys. Rev. Lett.* **102**, 180501 (2009).
 - [6] N. B. Lovett, S. Cooper, M. Everitt, M. Trevers and V. Kendon, *Phys. Rev. A* **81**, 042330 (2010).
 - [7] P. Zhang, B. H. Liu, R. F. Liu, H. R. Li, F. L. Li and G. C. Guo, *Phys. Rev. A* **81**, 052322 (2010).
 - [8] B. C. Travaglione and G. J. Milburn, *Phys. Rev. A* **65**, 032310 (2002).
 - [9] P. Xue, B. C. Sanders and D. Leibfried, *Phys. Rev. Lett.* **103**, 183602 (2009).
 - [10] P. Xue, B. C. Sanders, A. Blais and K. Lalumière, *Phys. Rev. A* **78**, 042334 (2008).
 - [11] P. Xue and B. C. Sanders, *New J. Phys.* **10**, 053025 (2008).
 - [12] W. Dür, R. Raussendorf, V. Kendon and H. J. Briegel, *Phys. Rev. A* **66**, 052319 (2002).
 - [13] M. A. Broome, A. Fedrizzi, B. P. Lanyon, I. Kassal, A. Aspuru-Guzik and A. G. White, *Phys. Rev. Lett.* **104**, 153602 (2010).
 - [14] F. Zähringer, G. Kirchmair, R. Gerritsma, E. Solano, R. Blatt and C. F. Roos, *Phys. Rev. Lett.* **104**, 100503 (2010).
 - [15] M. Karski, L. Förster, J.-M. Choi, A. Steffen, W. Alt, D. Meschede and A. Widera, *Science* **325**, 174 (2009).
 - [16] T. D. Mackay, S. D. Bartlett, L. T. Stephenson and B. C. Sanders, *J. Phys. A: Math. Gen.* **35**, 2745 (2002).
 - [17] A. Peruzzo, M. Lobino, J. C. F. Matthews, N. Matsuda, A. Polliti, K. Poulios, X. Q. Zhou, Y. Lahini, N. Ismail, K. Wörhoff, Y. Bromberg, Y. Silberberg, M. G. Thompson and J. L. O'Brien, *Science* **329**, 1500 (2010).
 - [18] T. A. Brun, H. A. Carteret and A. Ambainis, *Phys. Rev. A* **67**, 052317 (2003).
 - [19] Y. Omar, N. Paunkovic, L. Sheridan and S. Bose, *Phys. Rev. A* **74**, 042304 (2006).
 - [20] C. Liu and N. Petulante, *Phys. Rev. A* **79**, 032312 (2009).
 - [21] P. P. Rohde, A. Schreiber, M. Stefanak, I. Jex and C. Silberhorn, *New J. Phys.* **13**, 013001 (2011).
 - [22] M. Stefanak, S. M. Barnett, B. Kollar, T. Kiss and I. Jex, *New J. Phys.* **13**, 033029 (2011).
 - [23] S. D. Berry and J. B. Wang, *Phys. Rev. A* **83**, 042317 (2011).
 - [24] P. Xue and B. C. Sanders, *Phys. Rev. A* **85**, 022307 (2012).
 - [25] Y. Y. Xu, F. Zhou, L. Chen, Y. Xie, P. Xue and M. Feng, unpublished.
 - [26] F. M. Cucchietti, D. A. R. Dalvit, J. P. Paz and W. H. Zurek, *Phys. Rev. Lett.* **91**, 210403 (2003).
 - [27] A. S. Holevo, *Lect. Notes Math.* **1055**, 153 (1984).
 - [28] J. P. Keating, N. Linden, J. C. F. Matthews and A. Winter, *Phys. Rev. A* **76**, 012315 (2007).
 - [29] A. Schreiber, K. N. Cassemiro, V. Potoček, A. Gábris, I. Jex and C. Silberhorn, *Phys. Rev. Lett.* **106**, 180403 (2011).
 - [30] F. Helmer, M. Mariani, A. G. Fowler, J. von Delft, E. Solano and F. Marquardt, *Europhysics Letters* **85**, 50007 (2009).
 - [31] A. Blais, R. S. Huang, A. Wallraff, S. M. Girvin and R. J. Schoelkopf, *Phys. Rev. A* **69**, 062320 (2004).
 - [32] A. Blais, J. Gambetta, A. Wallraff, D. I. Schuster, S. M. Girvin, M. H. Devoret and R. J. Schoelkopf, *Phys. Rev. A* **75**, 032329 (2007).
 - [33] P. Xue, *Phys. Lett. A* **374**, 2601 (2010); P. Xue, *Chin. Phys. Lett.* **28**, 070305 (2011); P. Xue, *Chin. Phys. B* **20**, 100310 (2011).
 - [34] H. F. Wang, A. D. Zhu, S. Zhang and K. H. Yeon, *New J. Phys.* **13**, 013021 (2011).
 - [35] W. L. Yang, C. Y. Chen and M. Feng, *Phys. Rev. A* **76**, 054301 (2007).
 - [36] In this Sec., we only consider short time limit. That is we focus on the behavior of QW with decoherence for the first few steps.